

Approved for public release; distribution is unlimited.

Title:

CONTRIBUTIONS FROM THE MILAGRO
COLLABORATION TO THE XXVII INTERNATIONAL
COSMIC RAY CONFERANCE, HAMBURG, GERMANY

Author(s):

GALEN GISLER, NIS-2 TODD J. HAINES, P-23 CYRUS M. HOFFMAN, P-23 FRANK SAMUELSON,P-23 CONSTANTINE SINNIS, P-23

Submitted to:

XXVIITH INTERNATIONAL COSMIC RAY CONFERANCE AUGUST 7-15, 2001



Los Alarnos NATIONAL LABORATORY

Los Alarnos National Laboratory, an affirmative action/equal opportunity employer, is operated by the University of California for the U.S. Department of Energy under contract W-7405-ENG-36. By acceptance of this article publisher recognizes that the U.S. Government retains a nonexclusive, royalty-free license to publish or reproduce the published for finishing this contribution, or to allow others to do so, for U.S. Government purposes. Los Alamos National Laboratory requests that the publisher identify this article as work performed under the auspices of the U.S. Department of Energy. Los Alamos National Laboratory strongly supports academic freedom and a researcher's right to publish; as an institution, however, the Laboratory does not endorse the viewpoint of a publication or guarantee its technical correctness.



A Search for TeV Gamma-Ray Emission from Selected AGN Using Milagro

Wystan Benbow for the Milagro Collaboration

Santa Cruz Institute for Particle Physics, Univ. of California, Santa Cruz, CA 95064, USA

Abstract. The Milagro gamma-ray observatory, located near Los Alamos, NM, employs a water-Cherenkov technique to continuously monitor the northern sky for astrophysical gamma-ray emission near 1 TeV. Milagro's high duty-cycle (~95%) and wide aperture (~2 sr) allows for the detection of flaring behavior associated with TeV AGN, even during daytime transits. Results are presented from a search of the Milagro 2000-2001 data set for TeV emission from selected AGN, including the bright flare of Mrk421 in early 2001.

1 Introduction

The Milagro water-Cherenkov detector (60 x 80 x 8 m³) is an all-sky monitor sensitive to the extensive air showers (EAS) produced by gamma rays incident on the atmosphere in the energy range 200 GeV to 20 TeV. Milagro, which operates at 2630 m above sea level, employs two layers of submerged photomultiplier tubes (PMTs) to detect the Cherenkov light produced by secondary particles entering the covered reservoir of water. The first layer, consisting of 450 PMTs on a 2.8 x 2.8 m² grid under 1.5 m of purified water, utilizes the relative arrival time of the Cherenkov photons at the PMTs to reconstruct the direction of the incoming EAS with an accuracy of ~ 0.75 degrees. The second layer of 273 PMTs located at \sim 6 m depth is used to identify penetrating particles such as muons, hadrons and very energetic electromagnetic particles. Due to the low cross section for photo-production of hadrons, one expects many more muons and hadrons at

Correspondence to: Benbow (wrb@scipp.ucsc.edu)

ground level in an EAS initiated by a hadronic cosmic ray, allowing this second layer to be useful for determining the species of the primary particle. This is crucial for the detection of TeV sources, as the EAS initiated by hadronic cosmic rays greatly outnumber (\sim 10,000:1) those initiated by gamma rays. A rejection technique for Milagro, making use of this second layer has been developed, and is detailed in Sinnis *et al.* (2001). This technique has led to the detection of the Crab Nebula with a significance of 4.8 σ for the entire Milagro data set and confirms that the detector is performing as expected. A more detailed description of Milagro can be found in these proceedings (Sullivan *et al.*, 2001).

Milagro's ability to continuously monitor all sources in the overhead sky, even during daytime transits, makes it well suited for studies of AGN, which are known to be highly variable and exhibit flaring behavior. A smaller, less sensitive version of Milagro, known as Milagrito, detected the bright flare of Mrk 501 in 1997 (Atkins *et al.*, 1999). The improved sensitivity of Milagro, due to its larger effective area and the ability to reject some of the cosmic-ray background, enables it to observe similar phenomena with appreciable significance.

2 AGN Sample

Twenty-six AGN within the field of view of Milagro (0 < dec < 70) were selected for continuous observation. Only relatively nearby (z<.1) AGN are studied in order to minimize the attenuation of any potential signal by extragalactic background photons. This sample includes 3 AGN already detect-

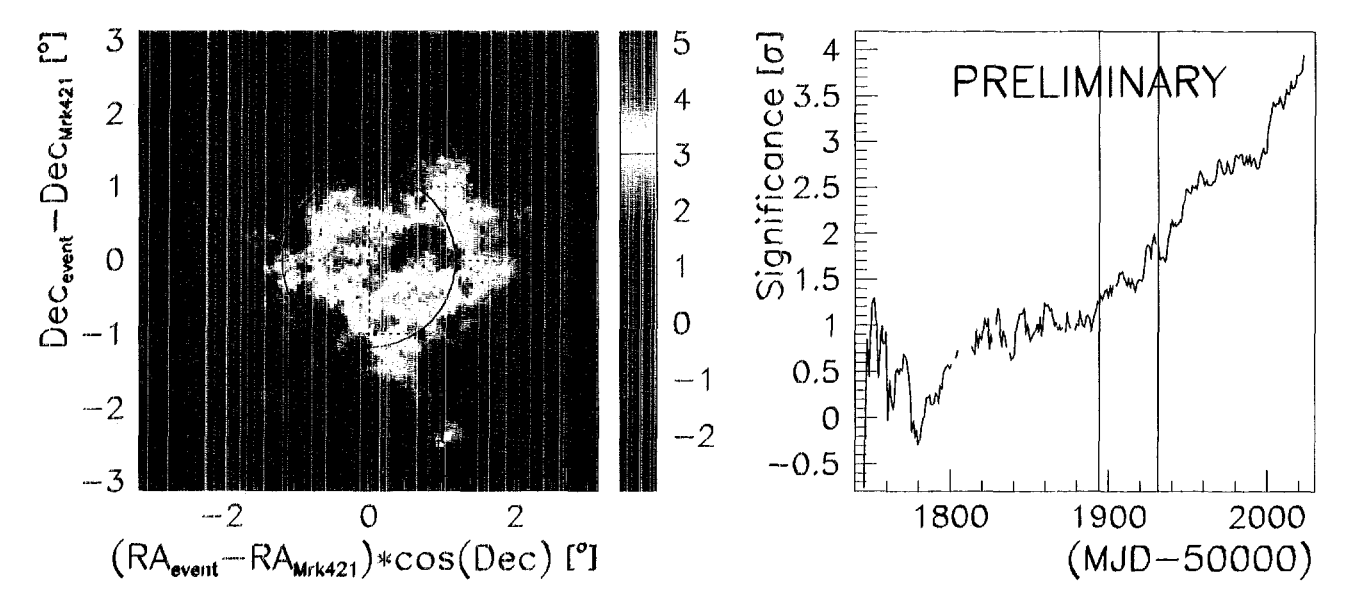


Fig. 1. On the left, a preliminary sky map of region centered on Mrk 421 for the period: June 14, 2000, to April 24, 2001. Neighboring points are highly correlated due to overlapping bins. The circle represents the bin size used for the analysis and is centered on the true position of Mrk 421. On the right, a preliminary plot of the accumulated Mrk 421 signal *vs.* time. The leftmost vertical line represents the date when the improved core reconstruction algorithm was implemented. The rightmost vertical line reresents the date the new calibrations were implemented. The date 1910 corresponds to January 1, 2001.

5 Data Set

Milagro began acquiring data in engineering mode on June 8, 1999, and has operated nearly continuously since January, 2000. As the understanding of the detector has increased, the online event reconstruction has undergone many changes. While many of these modifications are relatively minor, two of these have resulted in large increases in the detector's sensitivity. The first, occurring on June 14, 2000, involved implementing the background rejection algorithm online. Monte Carlo simulations indicate that this should result in an increase in sensitivity by a factor (Q factor) of 1.8(Sinnis et al., 2001). A new core reconstruction algoritm, implemented on December 15, 2000, constitutes the second major change. Monte Carlo simulations show that this change should result in an additional Q factor of 1.4. In addition, recent studies have improved the pulse height calibration of Milagro. These improvements affect both the hadron rejection and to a lesser extent the angular reconstruction of Milagro. More details can be found in Sinnis et al. (2001). Unfortunately, only limited raw data exists for events initially reconstructed in the vicinity of the candidate blazars. This does not allow for re-reconstruction of the data with the improved calibrations. However, as previously discussed raw data exists for events initially reconstructed in the vicinity of Mrk 421 during the time interval beginning January 17, 2001, to present. This data was reprocessed with the new calibrations, and is utilized in the analysis of Mrk 421. A consequence of these upgrades is that one must combine data utilizing varying calibrations and reconstruction techniques to study the AGN over larger time periods.

Milagro has detected the Crab Nebula with high significance by making use of the background rejection technique. Therefore, the Milagro data set from June 14, 2000, when the compactness parameter became part of the processed data, until April 24, 2001, was searched for TeV emission from the candidate blazars. This interval consists of 278 source transits. However, due to downtime for repairs and power outages, the effective exposure is actually 264 days. This time period includes the large flare of Mrk 421 in early 2001, as reported by HEGRA, Whipple and the RXTE All-Sky Monitor. The overall sample consists of XX.XXX billion events satisfying a trigger condition of at least ~ 50 top layer tubes hit within a window of 200 ns, taken at an average trigger rate between 1500 and 2000 Hz.

6 Results

6.1 Mrk 421

For the analyzed data set, Milagro detects an excess of 3337 ± 846 events from Mrk 421, corresponding to 4.0σ . The combined analysis cuts keep 11% of the events in the source bin. The left plot in Figure 1 is a sky map of detected significance for the region surrounding Mrk 421. Neighboring points on this map are highly correlated as the bins are overlapping. The right plot in Figure 1 shows how the significance at the position of Mrk 421 was accumulated. This preliminary result is consistent with expectations, and indicates that Milagro has detected Mrk 421 as a source of TeV gamma rays. The average rate of excess events observed is 12.6 ± 3.2 day $^{-1}$. Figure 2 shows the excess at the position on Mrk 421

divided by background for time interval studied. The data are binned in 30 day intervals, with the first and last points on the plot containing only 4 days each.

For comparison purposes, Milagro sees an excess from the Crab of 2134 ± 698 events, or 3.1σ during this time period. This is consistent with expectations and indicates that Mrk 421 produced an average flux level higher than the Crab for this data set. As expected, no flaring activity was detected for the Crab.

Results will be presented at the conference from the search for shorter timescale emission at Mrk 421's position.

6.2 Other AGN

Results will also be presented at the conference from the search for significant excess from the 25 other blazars for the entire time interval, as well as results from the short-term flare search.

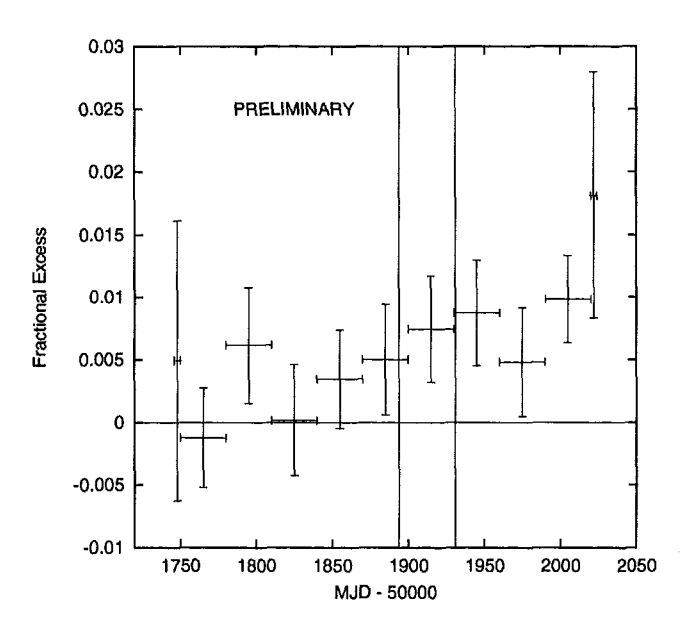


Fig. 2. Preliminary fractional excess vs. time from Mrk 421 as seen by Milagro. The leftmost vertical line represents the date when the improved core reconstruction algorithm was implemented. The rightmost vertical line reresents the date the new calibrations were implemented. The data are binned in 30 day intervals, with the first and last points containing only 4 days each. The date 1910 corresponds to January 1, 2001.

7 Conclusions

Milagro has detected Mrk 421 during its bright flare in early 2001. This, coupled with the detector's ability to monitor AGN during daytime transits, when observations with Air Cherekov Telescopes are impossible, shows that the Milagro gamma-ray observatory is poised to make significant contributions to the field of TeV astrophysics. The analysis of the signal from Mrk 421 is still ongoing. Thus, the results

presented in this paper are preliminary. Updated results, including the short-term flare search, will be presented at the conference for Mrk 421 and the other 25 AGN.

Acknowledgements. This research was supported in part by the National Science Foundation (Grant Numbers PHY-9722617, -9901496, -0070927, -0070933, -0070968, -0096256), the U. S. Department of Energy Office of High Energy Physics, the U. S. Department of Energy Office of Nuclear Physics, Los Alamos National Laboratory, the LDRD program at LANL, the University of California, the Institute of Geophysics and Planetary Physics, The Research Corporation, and the California Space Institute. We would also like to recognize the hard work of Scott Delay and Michael Schneider, whose dedication has been instrumental in operating Milagro. The author would also like to thank the American Astronomical Society for providing funding to attend this conference.

References

- D. Alexandreas et al., Point Source Search Techniques in Ultra High Energy Gamma Ray Astronomy, Nuclear Instruments and Methods in Physics Research Section A 328, 570-577, 1993.
- R. Atkins et al., TeV Observations of Markarian 501 with the Milagrito Water Cherenkov Detector, Astrophysical Journal Letters 525, L25-L28, 1999.
- R. Atkins et al., Milagrito, a TeV Air-Shower Array, Nuclear Instruments and Methods in Physics Research Section A 449, 478–499, 2000.
- M. Catanese et al., Discovery of Gamma-Ray Emission Above 350 GeV from the BL Lacertae Object 1ES 2344+514, Astrophysical Journal 501, 616-623, 1998.
- T. Li & Y. Ma, Analysis Methods for Results in Gamma-Ray Astronomy, Astrophysical Journal 272, 317–324, 1983.
- R. Mukherjee et al., EGRET Observations of High-Energy Gamma-Ray Emission from Blazars: an Update, Astrophysical Journal 490, 116–135, 1997.
- E.S. Perlman, X-ray Selected BL Lacs and Blazars, Proceedings of the GeV-TeV Gamma-Ray Astrophysics Workshop: Towards a Major Atmospheric Cherenkov Telescope VI, Snowbird, Utah, 53-65, August 13-16, 1999.
- M. Punch et al., Detection of TeV Photons from the Active Galaxy Markarian 421, Nature 358, 477-478, 1992.
- J. Quinn et al., Detection of Gamma Rays with E > 300 GeV from Markarian 501, Astrophysical Journal Letters 456, L83, 1996.
- C. Sinnis et al., these conference proceedings.
- G. Sullivan et al., these conference proceedings.



Search for Diffuse TeV Gamma-Ray Emission from the Galactic Plane, using the Milagro Gamma-Ray Telescope.

R. Fleysher for the Milagro Collaboration

Department of Physics, New York University, New York, NY 10003, USA

Abstract. Diffuse high energy gamma radiation can arise from a variety of astrophysical sources, in particular from interactions between energetic cosmic rays and matter in our galaxy. Emission from the galactic plane has been detected up to GeV energies by space-based detectors. Observations at higher energies, for which the flux is too low for satellites, can be done with ground based telescopes. Milagro is a wide-aperture extensive air shower water Cerenkov detector collecting data from a solid angle of about two steradians in the overhead sky at energies near 1 TeV. We have used a 2000-2001 data set from Milagro to search for the emission of diffuse gamma rays from the galactic disk. Preliminary results of the search will be presented.

1 Introduction

Cosmic rays are accelerated by unknown objects in our Galaxy and are trapped (for about 100 million years) by Galactic magnetic fields. The interaction of high energy cosmic rays with the interstellar material produces γ -rays by a combination of electron bremsstrahlung, inverse Compton and nucleon-nucleon processes. The nucleon-nucleon interactions give rise to π^0 's which decay to gamma rays and are expected to dominate the flux at energies above several GeV. In this manner, the regions of enhanced density (clouds of mostly atomic and molecular hydrogen) act as passive targets, converting some fraction of impinging cosmic rays into gamma rays. This should appear as a diffuse glow concentrated in the narrow band along the Galactic equator. Indeed, such an emission was detected by the space-borne detectors SAS 2, COS B (R.C. Hartman et al., 1979) and EGRET (S. D. Hunter et al., 1997) at energies up to 30 GeV.

However, observations with present satellite based instruments at higher energies are not possible due to the rapidly decreasing flux of γ -rays, requiring bigger effective area of

Correspondence to: R. Fleysher (roman.fleysher@physics.nyu.edu)

the detectors. Therefore, the use of ground-based arrays is needed to observe the diffuse Galactic radiation. Inasmuch as the Galactic cosmic ray spectrum extends beyond 10¹⁵ eV, the diffuse Galactic emission should extend well beyond the energy threshold of Milagro (~ 400 GeV). A number of authors have estimated the expected diffuse very high energy gamma-ray flux from the Galactic plane (see for example P. Chardonnet et al. (1995)): they generally predict a flux within $\pm 5^{\circ}$ of the Galactic equator in latitude that is $\sim 10^{-4} - 10^{-5}$ of the cosmic ray flux for the regions of the outer galaxy.1 The shape of the gamma-ray spectrum is predicted by the same authors as $\frac{dN}{dE} \sim E^{-2}$. However, at TeV energies the contribution from source cosmic rays, considered by E. G. Berezhko and H. J. Völk (2000), may increase the expected diffuse γ -ray flux by almost as order of magnitude compared to π^0 -decay model predictions. It is also possible that the spectrum of cosmic rays in the interstellar medium is substantially harder compared with the local one measured directly in the solar neighborhood (F. A. Aharonian and A. M. Atotan, 2000) which will lead to higher diffuse γ -ray flux as well.

At present, gamma rays from the galactic plane have not been detected above EGRET energies (only upper limits were set). The only measurements that approach the required sensitivity are above 180 TeV, performed by CASA-MIA experiment (A. Borione et al. , 1998). The best measurement in the 1 TeV region, which is two orders of magnitude less sensitive, is due to Whipple (P. T. Reynolds et al. , 1993). Milagro, the detector designed to cover the energy gap in the few TeV region between other existing instruments, should be able to detect the diffuse very high energy Galactic emission and possibly its spatial distribution and bring an enhanced understanding of Galactic cosmic rays. The sky coverage of Milagro is illustrated on Figure 1. Because Milagro is located in the northern hemisphere at latitude of 36°, the Galactic center is not in its field of view. However, a considerable portion

¹The outer Galaxy is defined as the region with galactic longitude l, $40^{\circ} < l < 320^{\circ}$.

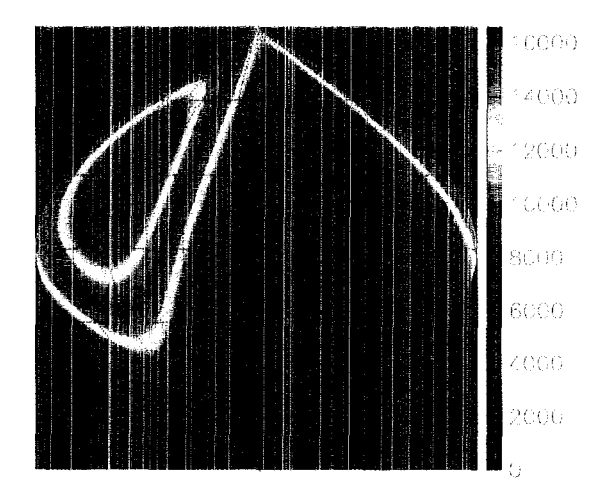


Fig. 1. The density of events from Milagro (in arbitrary units) plotted in galactic coordinate system, sine equal area projection. Grid lines are plotted every 30° in longitude and latitude. Galactic center is in the middle of the map

of the outer disk is visible to Milagro.

2 The Milagro Gamma-Ray Observatory

High energy gamma rays as well as cosmic rays do not penetrate the Earth's atmosphere, but interact at high altitude producing cascades of particles called extensive air showers. Milagro is the first detector designed to study air showers at energies near 1 TeV using water Cerenkov techniques by detecting particles in the cascade that survive to the ground level. The detector is built in the Jemez Mountains near Los Alamos, New Mexico, USA at an altitude of 2650 m. It presents a 60m x 80m x 8m pond, filled with clean water, covered with a light barrier and instrumented with 723 - 20 cm photo-multiplier tubes (PMT). The PMTs are arranged in two layers: top one of 450 tubes is used primarily to reconstruct shower direction, and the bottom one of 273 tubes is used for discrimination of gamma ray and hadron induced air showers. Milagro is currently operational. For a recent status update please see G. Sullivan et al. (2001).

The shower direction is calculated from the relative times at which the PMTs are struck after correcting for the effects of electronic slewing, sampling of particles in the shower front, and curvature of the shower front. After making these corrections, the direction of the shower plane can be determined with a χ^2 fit using the measured times and positions from the PMTs which also accounts for the tail of late light due to low-energy particles that tend to trail the shower front and nearly horizontal light in the water from the large Cerenkov angle and from scattering of particles and light in the

water. Baffles have been installed around the PMTs to block the horizontal light and increase the light collection.

3 Analysis Method

Most air showers detected are produced by charged cosmic rays that form an isotropic background. Emission from a gamma ray source would appear as an excess number of events coming from the direction of the source. Therefore, when searching for weak signals the analysis must be able to predict the expected number of air shower events at each candidate position assuming there is no source which then can be compared with the observed number of events to determine the excess. There are many effects in an air shower experiment that, if not handled properly, could cause possible large systematic errors leading to artificial creation or disappearance of sources. These effects include:

- -- times when the experiment was not operating
- non-uniformities in the acceptance of the array to air showers due to detector geometry
- short- and long-term event rate variations due to detector upgrades or changes in the atmosphere
- short- and long-term variations in the acceptance of the detector due to atmospheric conditions and detector reconfigurations.

These effects can cause variations in effective exposure of the array to different parts of the sky.

A method has been developed that is able to determine the number of expected background events at each point in the celestial sky, even though each of the above effects exists in the data, without having to make any cuts on the data. This technique is based on widely used method presented in (D. E. Alexandreas et al., 1993). The method takes advantage of the rotation of the Earth and is based on the assumption that the detector responds to an isotropic background of cosmic rays. Under this supposition there should be a time independent flux of particles from each direction in local coordinates. Thus, a shower detected with particular local coordinates could have arrived with equal probability at any other time of shower detection.

Each background event is generated from a real event by calculating new value of Right Ascension using new randomly chosen arrival time from the pool of registration times of collected events in a finite time window which is large compared to the source size convoluted with angular resolution. Inasmuch as events from the source region are used to estimate the background level, the background will be overestimated if the signal is indeed present. This leads to an underestimation of the signal strength. The time window, typically 2 hours for a point source search, is extended to 8 hours for this Galactic signal search to accommodate the 10 degree thickness of the disk.

However, the assumption of time invariance of the flux of detected cosmic rays is violated during such a long time period due to variations in the acceptance of the detector induced by atmospheric condition changes. The developed method is able to track and correct for such modulations. The extended version still possesses the advantages of the original one: background events have the correct distribution in local coordinates and it naturally compensates for event rate variations including interruptions of any length in data collection.

We are applying this analysis technique to search for a signature of gamma rays from the Galactic plane region at energies near 1 TeV in combination with the background rejection method presented at this conference (C. Sinnis et al., 2001) for improved sensitivity to diffuse Galactic gamma rays. Preliminary results will be presented at the conference.

Acknowledgements. This work is supported by the U. S. Department of Energy Office of High Energy Physics, the National Science Foundation (Grant Numbers PHY-9722617, -9901496, -0070927, -0070933, -0070968), the LDRD program at Los Alamos National Laboratory, Los Alamos National Laboratory, the University of California, the Institute of Geophysics and Planetary Physics, the Research Corporation, and the California Space Institute. We would also like to recognize the hard work of Scott Delay and Michael Schnieder, whose dedication has been instrumental in operating Milagro.

References

- F. A. Aharonian and A. M. Atotan, astro-ph/0009009, 2000.
- D. E. Alexandreas et al., Nuclear Instruments and Methods, A328, 570, 1993.
- E. G. Berezhko and H. J. Völk, Astrophysical Journal, 540, 923-929, 2000.
- A. Borione et al., Astrophysical Journal, 493, 175, 1998.
- P. Chardonnet et al., Astrophysical Journal, 454, 774, 1995.
- R.C. Hartman et al., Astrophysical Journal, 230, 597-606, 1979.
- S. D. Hunter et al., Astrophysical Journal, 481, 205, 1997.
- P. T. Reynolds et al., Astrophysical Journal, 404, 206, 1993.
- C. Sinnis et al., These Proceedings, 2001
- G. Sullivan et al., These Proceedings, 2001.

High Energy Solar Particles in the 6 November 1997 Ground Level Event

J.M. Ryan and the Milagro Collaboration

The large 6 November 1997 GLE was detected and its intensity measured by many neutron monitor stations. It was also registered in the Milagrito ground-level water-Cherenkov gamma-ray telescope. Atmospheric muons from solar energetic particles were detected within the 4800 square meter, 2650 m high pond over a period of several hours. The energy threshold for detecting a muon signal in Milagrito is greater than detecting a neutron signal in the nearby Climax NM, being a convolution of both the geomagnetic and atmospheric cutoffs. We estimate the onset of the signal to be at 1207 UT +/- 6 minutes, the same as that measured with NMs within measurement error. Based on the signal detected in a singles counter mode, we deduce from the relative signal strengths in neutron monitors and Milagrito an interplanetary proton rigidity spectrum that is rapidly softening above 4 GV. The spectral index above 4 GV is 9+/-2, as compared to that deduced purely from neutron monitors above 1 GV of 5.6+/- 0.4 (Lovell et al. 1999). Furthermore, we estimate that these protons and ions above 4 GV originated no lower (1 sigma) than 2 solar radii above the solar surface, suggesting the presence of intense shock at unusually low altitudes.

Milagro Detections of Solar Energetic Particles in the Current Solar Maximum

J.M. Ryan and the Milagro Collaboration

Milagro and its prototype predecessor Milagrito have been sensitive to interplanetary protons above 5 GV from October 1997 to the present, with one major interruption from March 1998 to March 2000 during which time Milagrito was decommissioned and Milagro was integrated. The smaller Milagrito detected the 6 November 1997 GLE while Milagro failed to register any signal from the far larger GLE of 14 July 2000. Both instruments operate(d) by detecting atmospheric muons generated by solar energetic protons interacting in the atmosphere. The two instruments possess(ed) a solar-proton energy threshold that is a convolution of the atmospheric cutoff (2650 m altitude) with the geomagnetic cutoff (3 GV). This combination of effects restricts their rigidity range to be above 5 GV approximately. Their effective areas grow rapidly with energy above 5 GV, becoming almost 1000 times larger at 10 GV than Climax is at the same energy. In a singles counter mode, random non-statistical fluctuations have the greatest influence on our sensitivity limit for detecting events. We present a summary of detections and non-detections of established GLEs and major flares.

The Cosmic Ray Moon Shadow Seen by Milagro

F. Samuelson for the Milagro Collaboration

Los Alamos National Laboratory

Abstract. The Milagro cosmic ray detector, a large-area extensive air shower (EAS) water Cherenkov experiment, easily detects the blockage of TeV cosmic rays by the moon. The absence of these cosmic rays can be used to calibrate the absolute energy scale and the directional event reconstruction of Milagro using the Earth's magnetic field as a magnetic spectrometer. These data can also be used to set limits on the antiparticle flux of TeV cosmic rays.

1 Introduction

Milagro is a large-area EAS water Cherenkov ground array located at Los Alamos National Laboratory at an atmospheric depth of 750 g/cm². There are two layers of photomultiplier tubes (PMTs), one under 1.35 meters of water and another below it under 6 meters of water. For this study only data from the top layer of PMTs are used. As in other EAS array experiments, the direction of an air shower is reconstructed using pulse times from the PMTs. The experiment is sensitive to airshowers with primaries from a few hundred GeV to 10's of TeV. For more information about the experiment see Sullivan (2001).

The Milagro experiment easily detects the blockage of cosmic rays by the moon. Figures 2 and 3 demonstrate this effect. As observed from the Earth the moon is approximately 0.52° degrees in diameter. Over the year and a half of operation Milagro has obtained 3776 hours of observation time on the moon when it was 15° or more above the horizon. In this time 2.81×10^5 events per square degree along the path traveled by the Moon triggered 45 or more PMTs in Milagro. Thus one expects the blockage of approximately 5.97×10^4 cosmic rays. Of these events, Milagro measures 5.5×10^4 missing events within 6° of the center of the moon's shadow (Figure 1). These numbers depend on the criteria used to select events.

Between the Earth and the Moon the paths of cosmic rays

panio or over

Correspondence to: samuelson@mailaps.org

bend due to the Earth's magnetic field. At the typical energies detected by Milagro, this deflection is around 0.6°c/TV . This deviation is useful in estimating Milagro's energy sensitivity and possibly differentiating particles from antiparticles, which bend in opposite directions in the Earth's magnetic field.

2 Map Creation and Background Estimation

To create a map in the region of a source in the celestial sky, the directions of reconstructed events are mapped according to some local two dimensional spherical coordinate system such as the equatorial coordinate system that uses hour angle and declination axes. A second map, which is rotated by the current hour angle of the celestial source with respect to the first map, is also created. As the hour angle of the source is continuously changing, this rotation is also changing. This second map is the source map, having its position constant with respect to the celestial source. If the first mapping is in equatorial coordinates then the second mapping is in celestial coordinates with axes of right ascension and declination. For our purposes the maps were approximated as two-dimensional histograms with $0.1^{\circ} \times 0.1^{\circ}$ bins, necessitating a change in the rotation angle between the two maps every 24 sidereal seconds.

To estimate the background in the source map, we divide the local coordinate map (the first map) by the number of events used to construct that map, giving a normalized probability distribution covering every point of interest on the local sky. This distribution is then convolved with the event rate as a function of the source's hour angle (or equivalently, sidereal time) to give give the expected background. This method is effectively similar to methods outlined in section 2.5 of Alexandreas (2001). For display purposes only, both the source and background map are smoothed by a uniform distribution of a size on the order of the point spread function.

Figure 2 shows a plot of the event excess in the vicinity of

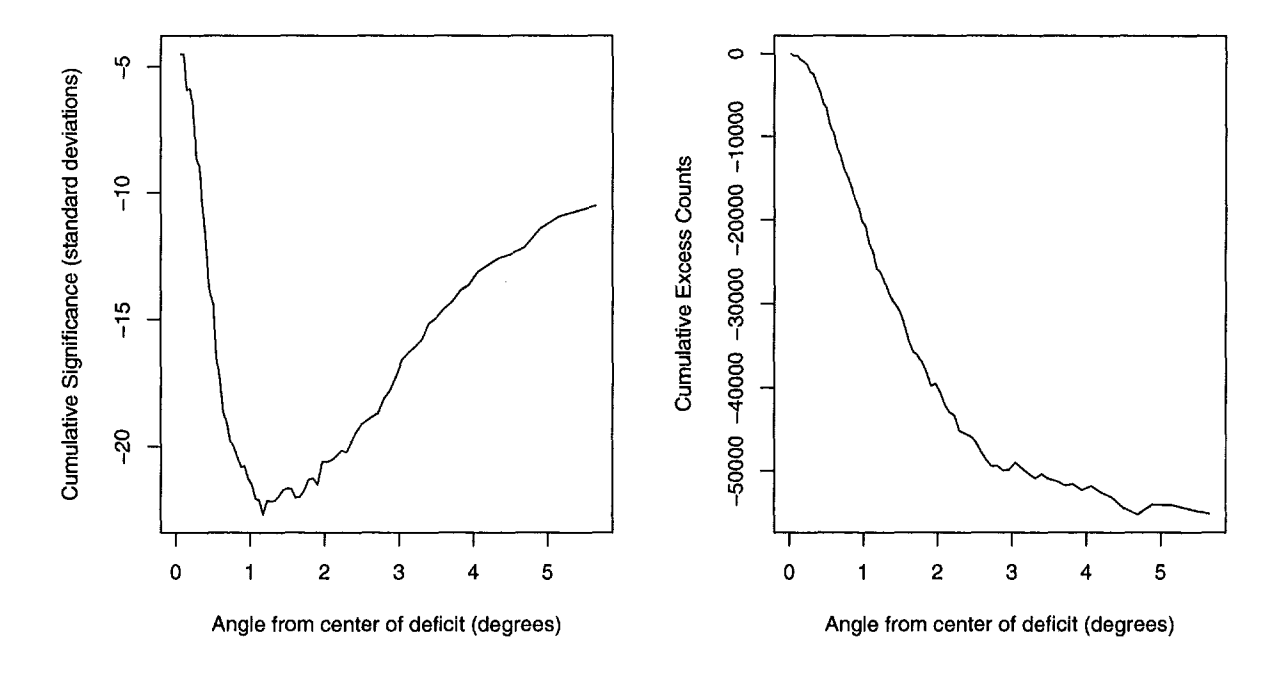


Fig. 1. Plots of cumulative excesses as a function of angle from the center of the deficit caused by the moon. The plot on the left is in units of standard deviations. The plot on the right is actual number of EAS events.

the moon using the above method exactly as outlined. Mapping the moon in this way has two drawbacks. First, in this plot all cosmic rays are not deflected in the same direction with respect to the moon due to the moon's motion through the sky with respect to the local magnetic field. This effect elongates the moon in the vertical direction. Second, the method outlined above includes the area around the moon in the estimation of the expected background of the moon. This is statistically incorrect. After a year and a half of operating Milagro the moon has blocked enough events that it is necessary to remove events in the region of the moon to correctly estimate the expected background. Including events from the region of the moon leads to an underestimate of the background along the strip of the moon's motion through the sky and a nonstatistical background distribution.

Figure 3 shows a rotated mapping where the expected cosmic ray deflection is along the abscissa. The expected direction of cosmic ray bending was calculated from a simulation that traced cosmic rays through the Earth's magnetic field (Wascko, 2001). These values were then used to rotate the map such that direction of magnetic deflection appears horizontal and to the left. The analysis in Figure 3 also removes the area around the moon from the calculation of its own background. A background is then calculated as before with a renormalization to the local event probability distribution. This correction is necessary for calculating the proper excesses as in Figure 1. Both corrections lead to a moon shadow that is more elliptical, elongated in the direction of

the magnetic deflections. The actual shape of the shadow with deflections at large angles from the moon becomes apparent.

3 Energy Calibration

Absolute energy calibration of EAS detectors is difficult, and relies on computer simulations of air showers. However, the blockage of cosmic rays by the moon and their deflection in the Earth's magnetic field provides Milagro with a simulation-independent energy calibration. The apparent deflection the moon's cosmic ray shadow from the position of the moon depends only on the Earth's magnetic field and the rigidity of the primary cosmic rays that trigger Milagro. If we take the Earth's magnetic field as a known quantity, and use the particle mass distribution around a TeV as measured by balloon experiments (Wiebel-Sooth, 2001; Asakimori, 1998), we can use the observed shadow deflection to constrain the median energy of the cosmic rays whose showers trigger Milagro.

The mean deflection of particles can be measured accurately, due to the large deficit caused by the moon. However, the deflection angle is relatively small ($\approx 0.4^{\circ}$) compared to the point spread function of Milagro, as can be seen in the Figures, and it is inversely proportional to the median rigidity of the cosmic rays that trigger Milagro (Wascko, 2001). Thus, small errors in the measured deflection lead to larger

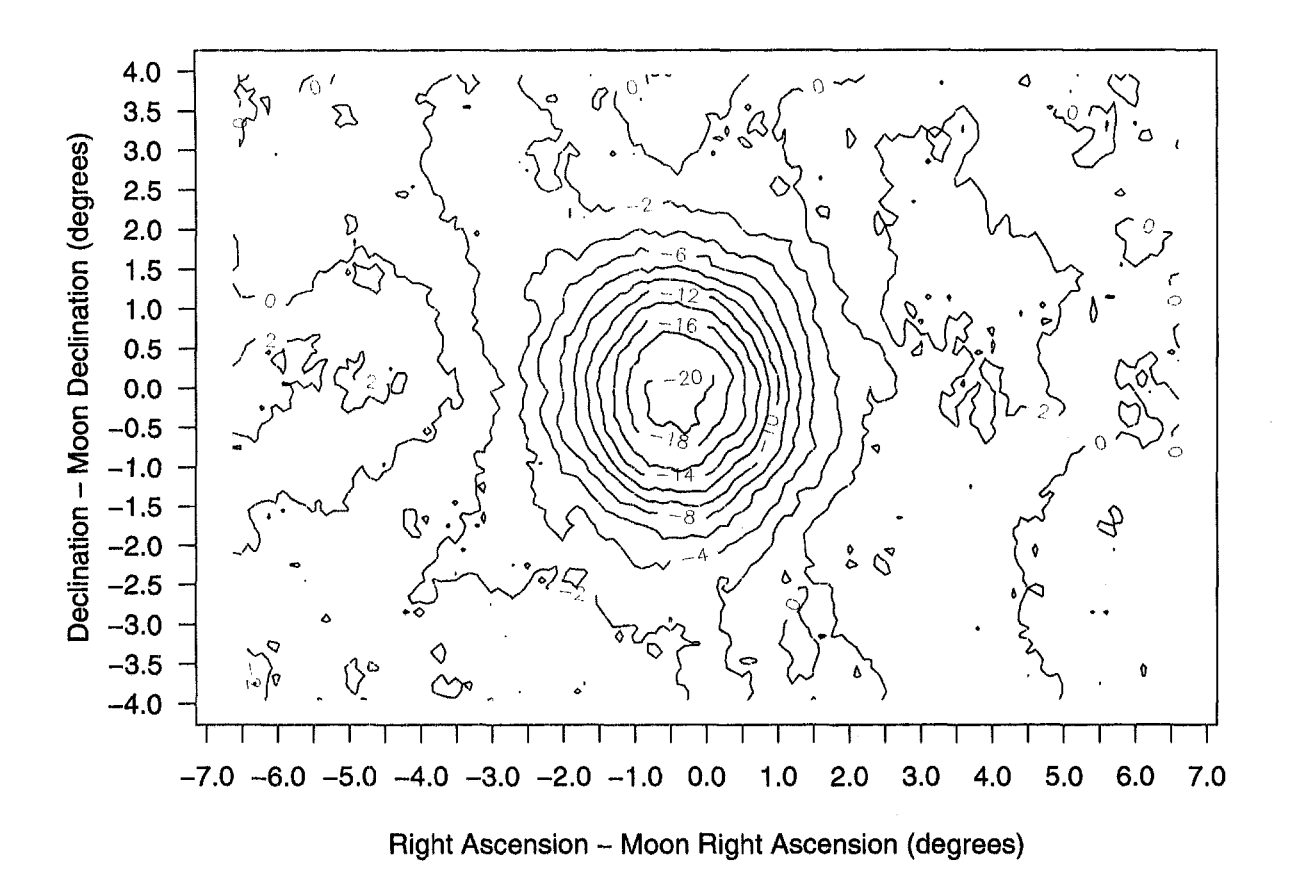


Fig. 2. Milagro event map of the region around the moon using right ascension and declination coordinates. Contours are labeled in units of standard deviations from a normal distribution. The estimated background used to make this map includes data from the region of the moon itself. This results in the small excesses seen to the left and right of the moon's position at 0 relative declination.

errors in median energy estimation. Given these limitations, we can set limits within a factor of 2 on the median energy of the cosmic rays that trigger Milagro. Better upper and lower limits will be presented at the conference.

4 Evaluating Event Reconstruction

Since the expected deviations due to the Earth's magnetic field lie along the abscissa in Figure 3, the vertical spread of the deficit in that plot should be due only to the point spread function of Milagro convolved with the shape of the moon itself. This allows us to set firm upper limits on the statistical error of EAS directional reconstruction ("pointing") by the Milagro array. When we deconvolve the moon from vertical spread of the deficit in Figure 3, we obtain a value of XX. The value obtained via this technique is an upper limit because the observed spread can only be worse than the statistical error of the pointing. We expect even better pointing on

astrophysical sources of gamma rays, as simulations indicate that gamma ray-initiated airshowers are better reconstructed than hadronic air showers due to their greater likelihood of triggering Milagro at small distances from the detector. This upper limit is consistent with another measurement of Milagro's statistical pointing error, Δ_{eo} (Atkins, 2000). A more exact upper limit on the statistical pointing error will be presented at the conference.

5 Antiparticle search

Just as we observe a shadow offset in the direction that we expect (to the left of the moon in Figure 3), we can search for a complimentary shadow due to antiparticles to the right of the moon. This problem is complicated by Milagro's large point spread function that smears the particle shadow across the moon's location. Such a search yields limits at around the 10% level. More accurate limits will be presented at the

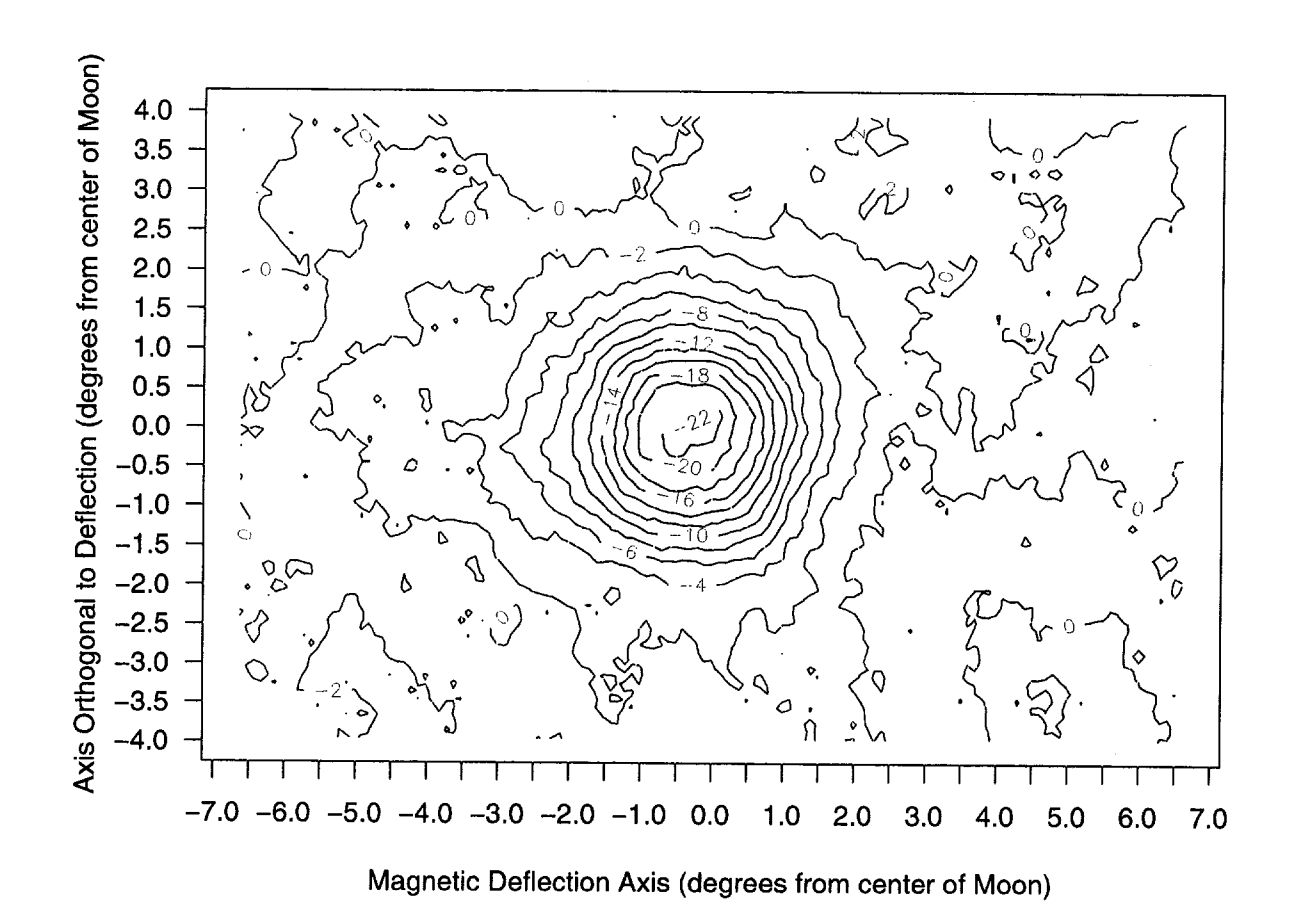


Fig. 3. Milagro event map of the region around the moon. Contours are labeled in units of standard deviations from a normal distribution. The expected cosmic ray deflections are to the left of the moon along the abscissa. The estimated background used to make this map excludes the region around the moon itself. Deflections at large angles to left are readily apparent.

conference.

Acknowledgements. This work is supported by the Department of Energy Office of High Energy Physics, the National Science Foundation (Grant Numbers PHY-9722617, -9901496, -0070927, -0070933, -0070968), the LDRD program at Los Alamos National Laboratory, Los Alamos National Laboratory, the University of California, the Institute of Geophysics and Planetary Physcis, the Research Coportation, and the California Space Institute. We would also like to recognize the hard work of Scott Delay and Michael Schnieder, without whom these data would not exist.

References

330, 389, 1998.

Asakimori, K., et al., Ap. J 502, 278, 1998.

Atkins, R. et al., NIM A, 449, p 478, 2000.

Alexandreas, at al. More stuff here.

Sullivan, G., et al., these proceedings, 2001.

Wascko, M.O., Ph.D. Thesis, University of California, Riverside, 2001.

Wiebel-Sooth, K., Biermann, P.L., & Meyer, H., Aston. Astrophys.

Background Rejection in the Milagro Gamma Ray Observatory

C. Sinnis for the Milagro Collaboration

Los Alamos National Laboratory

Abstract. Recent advances in TeV gamma ray astronomy are a result of the ability to differentiate between extensive air showers generated by gamma rays and hadronic cosmic rays. Air Cherenkov telescopes have developed and perfected the "imaging" technique over the past several decades, yet until now no method of background rejection has been successfully used in air shower arrays to detect a source of TeV gamma rays. The development of such a technique is necessary to improve the sensitivity of air shower arrays. We report on a method to differentiate hadronic air showers from gamma ray induced air showers in the Milagro gamma ray observatory. The technique is used to observe the Crab nebula at high significance (4.8σ) .

1 Introduction

Ground-based gamma ray astronomy was developed in the 1950's. Yet it was not until the late 1980's that the first source of TeV gamma rays was convincingly observed with a ground-based instrument. The innovation that changed the field was the development of a method to distinguish air showers induced by gamma rays and those induced by hadrons (protons and heavier nuclei), the so-called "imaging" technique. The imaging technique categorizes air showers by the shape and orientation of the Cherenkov light pool as observed in the image plane of an air Cherenkov telescope (Hillas 1985). This technique was used by the Whipple experiment to detect TeV gamma ray emission from the Crab nebula, the first detected source of TeV photons. Since the initial discovery of the Crab at least 5 other sources of TeV gamma rays have been detected (Hoffman et al. 1999, Ong 1998, Weekes 2000). Despite the recent success of imaging air Cherenkov telescopes, they have several limitations. Since they are optical instruments they can only observe the sky on clear, dark (moonless) nights (the typical duty cycle of these instruments is between 5 and 10%), and they can only observe a small fraction of the sky at any one time (of order 4×10^{-3} sr). In contrast, a detector that detects the particles in the air shower that reach the ground, known as an extensive air shower (EAS) array, can operate 24 hours/day, and can simultaneously view the entire overhead sky. Past efforts to distinguish hadronic and gamma ray induced air showers in EAS arrays have relied on the identification of muons. At energies above 100 TeV the CASA and CYGNUS arrays used shielded detectors to identify muons present in hadronic air showers. While the CASA array achieved very high levels of background rejection (rejecting 94% of the cosmic ray background above 115 TeV, and 99.93% of the background above 1175 TeV, while retaining over 72% of the gamma ray signal), no signals were observed in their data (Borione et al. 1997). It is generally believed that the absence of sources at these high energies is due to the absorption of high-energy photons by the cosmic background radiation and the steeply falling spectra of astrophysical sources. The Milagro detector is sensitive to much lower energy primary photons (\approx 500 GeV) and can therefore see sources at much greater distances (redshift ≈ 0.1). Here we report on the development of a technique to reject the hadronic background in Milagro. We demonstrate the efficacy of the technique with a detection of the Crab nebula and discuss possible improvements in the technique.

2 The Milagro Detector

The Milagro TeV gamma ray observatory is described in detail elsewhere in these proceedings (Sullivan *et al.* 2001). Milagro has 723 photomultiplier tubes (PMTs) submerged in a 6-million gallon water reservoir. The detector is located at the Fenton Hill site of Los Alamos National Laboratory, about 35 miles west of Los Alamos, NM, at an altitude of 8600' (750 g/cm²). The reservoir measures 80m x 60m x 8m (depth) and is covered by a light-tight barrier. The PMTs are secured to a grid of sand-filled PVC sitting on the bottom of the reservoir by a Kevlar string. The PMTs are arranged

in two layers, both on a 2.8m x 2.8m grid. The top layer of 450 PMTs (submerged under 1.35 meters of water) is used primarily to reconstruct the direction of the air shower. By measuring the relative arrival time of the air shower across the array the direction of the primary cosmic ray can be reconstructed with an accuracy of roughly 0.75°. The bottom layer of 273 PMTs (submerged under 6 meters of water) is used primarily to discriminate between gamma ray initiated air showers and hadronic air showers.

2.1 Identification and Rejection of Hadronic Events

It is well known that EAS induced by hadronic cosmic rays contain many more muons (from pion decay) and hadrons than EAS induced by gamma rays of comparable energy. In Milagro, the top 6 meters of water effectively absorb the electromagnetic component of the air showers and we identify hadronic events by looking for bright, compact clusters of light in the bottom layer. Using Monte Carlo simulations we estimate that 79% of all proton showers that trigger Milagro contain a muon and/or a hadron that enters the pond, while only 6% of gamma ray induced air showers contain a muon and/or a hadron that enters the pond. The trigger threshold in the simulation was set to 50 PMTs, the nominal hardware trigger requirement in Milagro.

The parameter used to differentiate hadronic showers is

$$C = \frac{NB_2}{MaxB} \equiv Compactness \tag{1}$$

where NB_2 is the number of PMTs in the bottom layer with more than 2 photo-electrons (PEs) and MaxB is the maximum number of PEs in any PMT in the bottom layer. Small bright clumps on the bottom will give small values of compactness, while showers that uniformly illuminate the bottom with small hits will give large values of compactness. Figure 1 shows the compactness distributions for Monte Carlo proton showers, Monte Carlo gamma showers, and for data. One sees a clear difference between Monte Carlo gamma ray showers and proton showers. Overall the data matches the Monte Carlo proton distribution reasonably well. Beyond a value of $C \approx 2.5$ one can see a discrepancy between the data and the Monte Carlo proton showers. This discrepancy is due to problems in the pulse height calibration of the detector and is being corrected (see the appendix).

If all events with $C \leq 2.5$ are removed (identified as hadronic), we should retain 54% of the gamma ray events and only 9% of the proton events. This results in an improvement in sensitivity of 1.8. This is often referred to as the Q factor of the cut.

We should note that even for events where no muons or hadrons enter the pond there is an observable difference between air showers induced by hadrons and those induced by gamma rays. Using the same cut on the compactness parameter ($C \le 2.5$) the Monte Carlo predicts a Q factor of 1.2 for these events (retaining 54% of gamma ray events and 20% of proton events). Examination of the electromagnetic particles that strike the pond shows that they tend to be more energetic

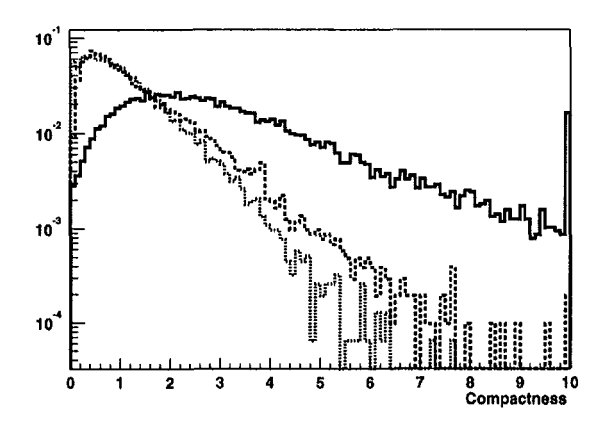


Fig. 1. The compactness distribution for Monte Carlo gamma rays (solid line) Monte Carlo protons (dashed line) and data (dotted line).

and more clumped in hadronic showers than in gamma ray induced showers.

2.1.1 Energy Dependence of Compactness Cut

When analyzing astronomical signals it is important to understand the energy dependence of the instrument. In particular this includes the energy response of any cut performed upon the data. An ideal cut would have an efficiency for signal events that is independent of the energy of the primary gamma ray. In practice such uniformity of response may be difficult to achieve. In Figure 2 we show the efficiency of the compactness cut as a function of primary gamma ray energy. The cut reaches 50% efficiency at ~1.5 TeV. This is below the median energy for gamma ray showers ($E^{-2.4}$ spectrum) that trigger Milagro and get reconstructed into a 2.1° square bin around the source (3.5 TeV). After the compactness cut is applied the median energy rises to 4.7 TeV. Note that the compactness cut is relatively uniform for proton events, while it is a relatively strong function of energy for gamma rays. Since the significance of a signal is inversely proportional to the square root of the background we can conclude that the observed improvement in sensitivity is not due to the energy dependence of the cut (for all sources with differential energy spectra steeper than $E^{-2.7/2}$).

3 Application to the Crab Nebula

As a test of the background rejection method we apply it to a search for TeV gamma rays from the Crab nebula. The Crab nebula was first detected at TeV energies in 1989 (Weekes et al. 1989). Since that time it has become the standard reference of TeV gamma ray astronomy. With a steady flux of $3.2 \times 10^{-7} (E/TeV)^{-2.49} \ \mathrm{m^{-2}s^{-1}TeV^{-1}}$ (Hillas et al., 1998) it is useful for cross calibrating the sensitivity of different instruments.

The dataset begins on June 8, 1999 and ends on April 24, 2001. Because of detector down time and periods of running

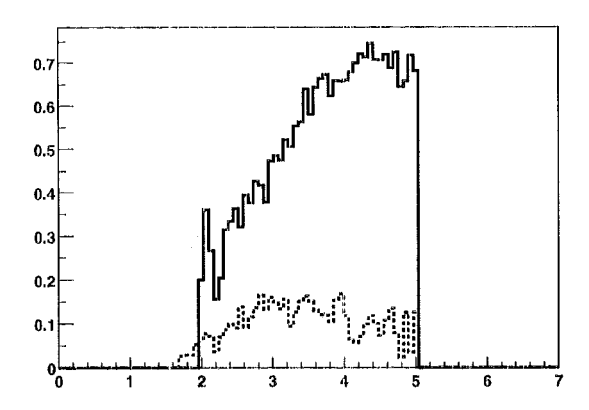


Fig. 2. The energy dependence of the compactness cut. The fraction of gamma ray events (solid line) and proton events (dashed line) retained is shown as a function of primary gamma ray energy in TeV.

at a lower rate (this data includes the time period when the detector first began taking data and was operating in an engineering mode) the effective exposure of this time interval is roughly 1.35 year of running in our current mode. During this interval we accumulated 50.261 billion events. The results of the Crab analysis are given in Table 3. We give the results for the raw data and for the data after the compactness cut has been applied. From these results we see a realized O factor of 4.8, consistent with Monte Carlo expectations (the error on the observed ratio is asymmetric and driven by the 1σ uncertainty in the denomintaor). The observed discrepency between the measured Q factor and the predicted Q = 1.8 is due to the observed excess with no background rejection cut applied to the data. Monte Carlo simulations indicate that we should observe a 2.7σ excess with no cuts and 5σ excess with the background rejection cuts. This cut removes 91% of the data, consistent with the Monte Carlo prediction of 90% rejection. A clear signal with a significance of 4.8σ is observed with the compactness cut. Since this data was obtained we have improved the pulse height calibration (see Appendix A) of the detector and we expect the details of the result to change. Updated results will be presented at the conference. Figure 3 shows a map of the statistical significance of the excesses in the region around the Crab nebula. At each point we plot the significance of any excess (or deficit) in a 2.1 degree square bin, centered on the bin position. The bin size used is shown as a circle in the figure. The Crab is at the center of the sample bin shown. The left-hand plot shows the significance before the application of the background rejection. The plot on the right shows the significance after the requirement C > 2.5 has been applied to the data.

4 Future Improvements

The algorithm described above is quite simple, depending only on the ratio of two quantities, independent of the event size or other characteristics. Monte Carlo simulations indicate that this simple ratio is not independent of other measured quantities in Milagro. Compactness for both gamma rays and protons is a function of the number of PMTs in the bottom layer with more than two PEs. For example, on small events with only a few PMTs illuminated in the bottom layer the compactness parameter may be quite small even if the pulse height in the brightest PMT in the bottom layer is below 8 PE. While these events would be rejected as hadronic events Monte Carlo simulations indicate that they are most certainly gamma ray events. Similarly for very large events with the core on the pond, gamma ray showers will be mistaken for hadronic events. However, a hadronic core deposits much more energy in the pond than does an electromagnetic core. By examining the full two-dimensional space of MaxB vs. NB_2 we should be able to improve the background rejection in Milagro. Using the Monte Carlo we derive the probability that a gamma ray or proton event will fall at a given point in this space. We use the MARS algorithm developed by J. Freidman (Freidman 1999) to fit these probability densities to a set of spline basis functions. For each point in this space we calculate the ratio of the probability for a gamma ray and a proton to fall at that point in the space (P_{γ}/P_{proton}) . We than find the distribution of P_{γ}/P_{proton} for all gamma ray and proton events. The optimal value of P_{γ}/P_{proton} at which to cut the data is determined by maximizing the signal to noise level $(F_{\gamma}/\sqrt{F_{proton}})$, where F is the fraction of events retained). By excluding all events with $\ln(P_{\gamma}/P_{proton}) < 2.0$ we remove 88% of the simulated proton events and retain 68% of the gamma ray events, for a predicted quality factor of 2.2 a 20% improvement over the simple compactness cut. An analysis of the Crab data with this cut yields similar results (4.8 σ) to the simple compactness cut, consistent with the expected improvement.

5 Conclusions

The bottom layer of Milagro is a coarse imaging calorimeter and can be used to measure the distribution of energy deposited in Milagro. Hadronic cosmic rays generate air showers with penetrating particles that deposit localized clumps of energy in the Milagro detector. We have developed a simple and fast algorithm to differentiate air showers induced by hadronic cosmic rays from those induced by gamma rays. This simple cut based on a compactness parameter improves the sensitivity of Milagro by a factor of 1.8. We have used this cut to observe TeV gamma ray emission from the Crab nebula. This is the first demonstration of the ability of an EAS array to reject hadrons and enhance the significance of an observation of a source of TeV gamma rays. We are currently investigating more sophisticated techniques that utilize more information to improve our background rejection capabilities. As Milagro is a new and unique type of instrument we are only beginning to understand its response to cosmic rays and gamma rays. As our understanding of this new instrument improves we expect to further improve the sensitiv-

Data Selection	ON Source	OFF Source	Excess	Significance
All Data	8,749,562	8,746,621	2941	1.0 σ
Compactness > 2.5	787,503	783,059	4444	4.8 σ

Table 1. Observed excess from the Crab nebula, using all the data and data after the background rejection is applied.

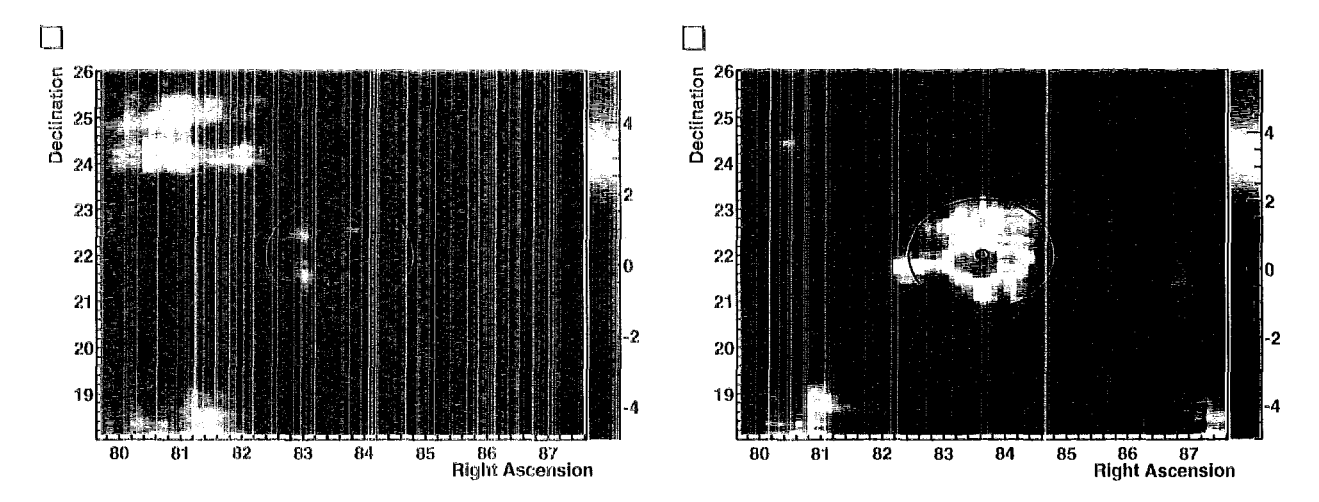


Fig. 3. Significance map of the region around the Crab nebula. The plot on the left shows the significance of all the data (no cut on the compactness). The plot on the right shows the significance after the compactness cut (C>2.5) is imposed on the data.

ity of Milagro.

Acknowledgements. This work is supported by the Department of Energy Office of High Energy Physics the National Science Foundation, the LDRD program at Los Alamos National Laboratory, Los Alamos National Laboratory, the University of California, the Institute of Geophysics and Planetary Physics, the Research Coportation, and the California Space Institute. We would also like to recognize the hard work of Scott Delay and Michael Schnieder, whose dedication has been instrumental in operating Milagro.

Appendix A Pulse Height Calibration of Milagro

Milagro uses the time-over-threshold (TOT) technique for measuring the pulse height at each PMT. For a exponential pulse one expects the following relationship between TOT and pulse height measured in PEs: $PE = \alpha e^{TOT/\beta}$, where β is the shaping time of the electronics and α is a gain dependent normalization. Thus, the error in the measured pulse height is exponentially dependent upon the error in the measurement of the TOT. In Milagro there can be a significant amount of late light within the detector (due to large angle particles, light reflected from the cover, and scattered light), resulting in large errors in the measurement of TOT. We have minimized this effect by implementing two thresholds on every electronic channel. The first threshold is set at ≈ 0.25 PEs and the second to ≈6 PEs. Since late light tends to be in the single PE range the higher threshold is relatively immune to mis-measurements of the pulse height, until up to large values of pulse height. Near threshold the TOT technique has a resolution of $\approx 8\%$ (see Atkins *et al.* 2000).

The initial pulse-height calibration of Milagro used the

TOT from the low threshold discriminator up to pulse heights of 15-30 PEs. The late light in the detector causes these measurents to have relatively poor resolution \approx 20%. The distribution is asymmetric, with the error typically being to measure a pulse height larger than the true pulse height.

The background rejection technique described in this paper is inherently sensitive to such errors for two reasons:

1) The pulse height range of 8-20 PE is the range of pulse heights that a muon produces in the bottom layer and 2) By selecting the PMT with the maximum value one is most likely to select the PMT that mismeasured the pulse height. We have recently developed a method that allows us to utilize the laser calibration system to obtain reliable pulse-height calibrations for small values of the high threshold TOT, corresponding to 6-10 PEs. This will significantly improve the pulse-height resolution in this critical region.

References

Atkins, R. et al., NIM A, 449, p 478, 2000.

Borione, A., et al., Phys Rev D, 55, p 1714, 1997.

Freidman, J. H., Annals of Statistics, 19, Issue 1, p 1, 1999.

Hillas, A.M., Proc. 19th ICRC (La Jolla), 3, 445, 1985.

Hillas, A.M., et al., Astrophys. J., 503, p 744, 1998.

Hoffman, C. M., Sinnis, C., Fleury, P., and Punch, M., Rev Mod Phys, Vol. 71, No. 4, p 897, 1999.

Ong, R., Phys. Rep., 305, p 13, 1998.

Sullivan, G., at al., these proceedings, 2001.

Weekes, T. C., et al., ApJ, 342, 379, 1989.

Weekes, T. C., Physica Scripta, T85, p 195, 2000



A Search for Bursts of TeV Gamma Rays with Milagro

A.J. Smith for the Milagro Collaboration

University of Maryland, College Park

Abstract. The Very High Energy (VHE, E > 100 GeV) component of Gamma-Ray Bursts (GRBs) remains unmeasured, despite the fact that models predict that the spectrum of GRBs extends beyond 1 TeV. Satellite detectors capable of observing GRBs lack the sensitivity to detect γ -rays with energies greater than ≈ 30 GeV due to their small effective area. Air Čerenkov telescopes, capable of detecting TeV point sources with excellent sensitivity have limited sensitivity to GRBs due to their small fields of view and limited duty cycles. The detection of TeV emission from GRBs is further complicated by the attenuation of infrared VHE photons by interaction with the intergalactic infrared radiation. This process limits the horizon for TeV observations of GRBs to z < 0.3 or less. As only about 20 GRBs have well measured redshifts, the fraction of GRBs close enough to observe at TeV energies remains unknown. The Milagro Gamma Ray Observatory began operation in June 1999. The detector consists of a large man made pond (4800 m²) instrumented with an array of photo-multiplier tubes. Milagro operates 24 hours a day and continuously observes the entire overhead sky (≈2 sr). Because of its wide field of view and high duty cycle Milagro is uniquely capable of searching for TeV emission from GRBs. An efficient algorithm has been developed to search the Milagro data for GRBs with durations from 250us to 40s. The search, while designed to search for the TeV component of GRBs, may also be sensitive to the evaporation of primordial black holes, or some yet undiscovered phenomenon. The results of this search are presented.

1 Introduction

Despite the fact that 3 decades have past since their discovery, the source GRBs remains unclear. The spectrum of GRBs above the 30 MeV has only been measured for a few very bright bursts within the field of view of the EGRET detector (Esposito 1999,D). At energies beyond the reach of EGRET, E > 100 GeV, high sensitivity measurements have not been made. It is widely believed that the γ -ray radiation from GRBs detected in the 30 keV to 1 MeV range is due to synchrotron radiation from a population of very high energy electrons. Alternatively, the electron population could lose their energy via inverse Compton (IC) scattering off of synchrotron photons (or photons from an external source) producing a very high energy IC γ -ray component along with lower energy synchrotron γ -rays. Several models of GRB origins predict TeV scale radiation (Dermer, Böttcher and Chiang 2000) from the IC process with comparable fluence to the well measured MeV scale radiation. Measuring the VHE component of GRBs may be critical to the understanding of the environment of the charged particle acceleration.

The difficulty of measuring the TeV component of GRB radiation is complicated by the fact that VHE radiation is attenuated by infrared (IR) photons. Both IR photons from the vicinity of the origins of the burst and the intergalactic IR background radiation can dissipate the VHE γ -ray component of the GRB spectrum. While the IR photon density in the vicinity of the burst is unknown, the intergalactic IR background is well modeled. Attenuation of VHE γ -rays from this source is likely to limit the horizon of VHE measurements to $z\approx 0.3$.

One approach to searching for VHE emission from GRBs is to search bursts in the Milagro data that are coincident in time and direction as GRBs detected by the BATSE experiment (Paciesas 1999), or another GRB monitor. The Milgrito experiment, a predecessor to Milagro, observed evidence for TeV emission from from GRB970417a in a search conducted for GRBs coincident with the BATSE detector (Atkins et al, 2000). But since the loss of BATSE, due to the de-orbit of the Compton Gamma-ray Observatory, there is no all-sky GRB monitor with a high sensitivity. The rate of satellite observations of GRBs within Milagro's field of view has dropped from one per week when BATSE was active to less than one per month for the existing GRB sensitive satellites. For this reason, it is important to conduct a search for GRBs in the Milagro data without the constraint that the burst be coincident with a satellite GRB detector

2 The Milagro Detector

The Milagro Detector (Sullivan 2001) is an air-shower array that employs a man large man-made pond of water instrumented with photo-multiplier tubes (PMTs) to detect Cerenkov radiation from secondary shower particles in extended air showers. The detector is located in the Jemez Mountains near Los Alamos, New Mexico at an altitude of 2600m (750g/cm² of overburden). The detector consists of a rectangular reservoir measuring 80m x 60m and 8m deep instrumented with 2 layers of PMTs. The PMTs are secured to a grid of sand filled PVC pipes that covers the bottom of the reservoir. The top layer contains 450 PMTs distributed in an 25 x 18 grid at a depth of 1.4m and is used primarily for measurement of the arrival times of secondary shower particles. The bottom layer contains 273 PMTs on a smaller 19 x 13 grid at a depth of 6m. This deep layer provides a calorimetric measurement of secondary shower particles and is used to distinguish deeply penetrating muons and hadrons, common in hadron induced air showers, from electrons and γ -rays. Simple cuts on measured quantities in the bottom layer allow for the removal of > 90% of the hadronic background while preserving > 60%of γ -ray induced showers increasing the sensitivity of the detector by a factor of ≈ 1.8 . The technique has been verified through observations of MRK-421 (Benbow 2001) and the Crab nebula (Sinnis 2001).

Milagro is operated with a trigger that requires roughly 50 PMTs to be hit within a 200ns time window. Under normal operating conditions, this trigger will provide about 1500 triggers/sec. In winter months when snow accumulates on the cover, slightly increasing the detector's overburden, the trigger rate is lower. When the cover is raised and separated from the surface of the water, the reflective properties of the surface change and the trigger rate increases.

3 Searching for GRBs

The goal of this work is to conduct a search for GRBs in the vast Milagro data set without the any initial knowledge of

the GRBs position in the sky, start time or duration. Milagro has only limited γ -hadron separation, so γ -ray sources are identified as non-statistical excesses on top of an isotropic background of cosmic-ray hadrons. The task of searching the Milagro data, which contains more than 50 Billion events, is computationally challenging.

The search of the data a fundamentally simple binned analvsis. The events collected for a candidate start time and duration, are binned into a fine, $0.2^{\circ} \times 0.2^{\circ}$, map in Hour Angle (HA) and declination (δ). For each position on the fine grid, all the neighboring bins within $\frac{1.0^o}{cos\delta}$ in HA or 1.0^o within δ are summed to give the number of measured events at the candidate position. The sum corresponds to a 2.2° square bin which was determined with simulations to be roughly optimal for point source searches in the Milagro data. The background is then estimated from data collected in the half hour prior to the GRB candidate time, and the Poisson probability that the number of measured events, or more, is observed given the measured background is calculated. All the points within the fine map with zenith angle less than 45° are considered. Finally, the candidate start time is advanced by 10% and the procedure is repeated. This procesure is independently performed for 27 candidate GRB durations ranging from $250\mu s$ to 40s distributed uniformly in log(Duration), with each subsequent candidate duration 58% longer than the last. This procedure employs a high degree on overlap spatially, temporally and in candidate duration maximizing sensitivity to bursts of unknown time and position.

The search was conducted using two nearly identical algorithms. One optimized for the case where the search region has a low event density and the other for regions with a high event density. For the former case a table of candidate search positions is constructed by considering only those positions in the vicinity of at least two events. In cases where the average number of events in the signal bin is low (<<1), this method is considerably faster than just a simple grid search. When the event density is high (> 2), most positions in the sky are included in the candidate table, and the overhead of constructing the table of candidate positions slows down the search. In this case a second search algorithm is used. The second algorithm performs a relatively coarse search on a $0.6^{\circ} \times 0.6^{\circ}$ degree grid, one third the density of the final search. If a GRB candidate position is located using the coarse search that yields an excess with Poisson probability less than 10^{-4} , the eight nearest neighbor bin surrounding the candidate source position are subsequently searched. The loss in sensitivity from not searching the entire sky with the finer (0.2°) binsize is negligible, because a probability threshold of typically $P_{Poisson} < 10^{-13} (7.5\sigma)$ is required to identify an excess as a GRB, and the coarser search will always yield a probability less than 10^{-4} in the vicinity of such an excess.

Figure 1 shows the distribution of Poisson probabilities for 5 of the 27 GRB candidate durations searched for 6 months of Milagro data collected between September 14, 2000 and April 28, 2001. The figures show a that the frequency of a probability decreases, as is should, by 1 decade for each

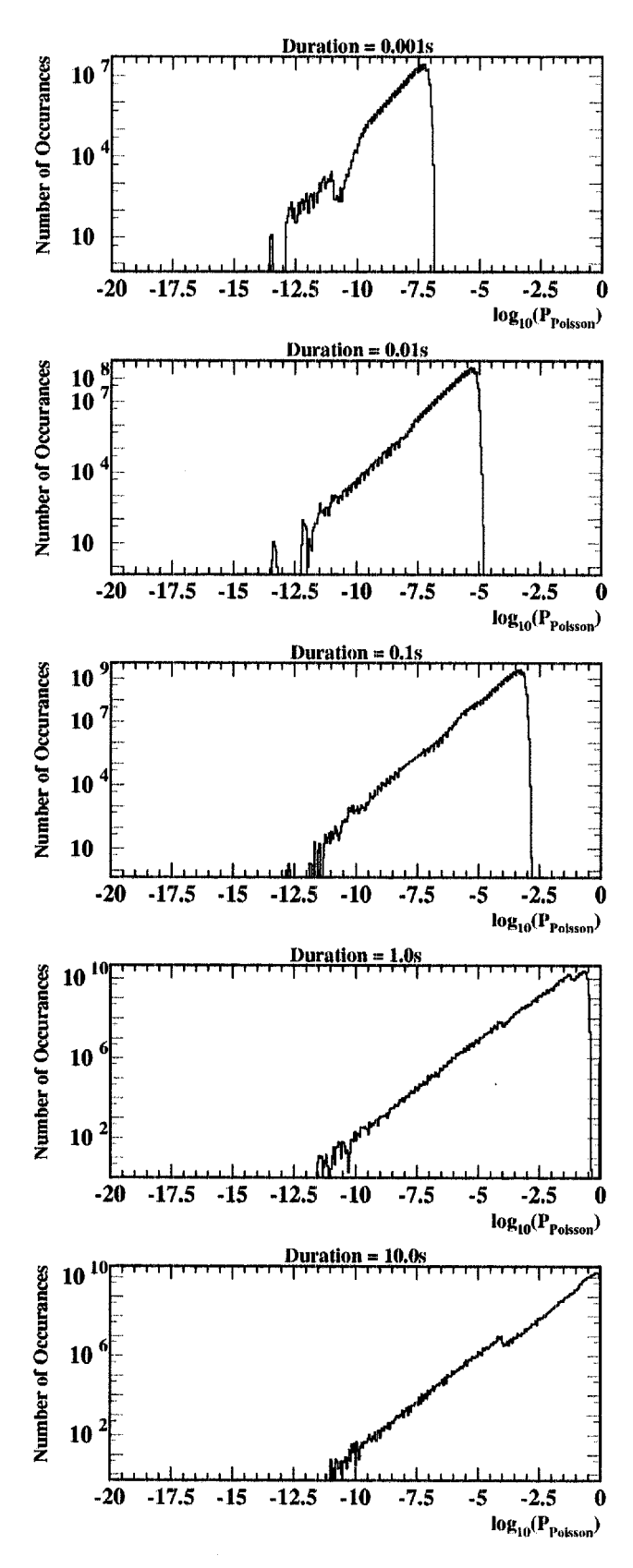


Fig. 1. Probability distributions for 5 of the 27 GRB candidate durations.

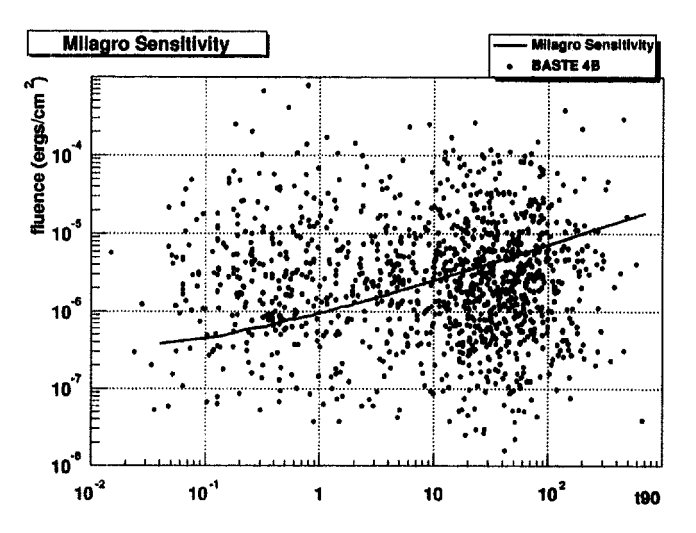


Fig. 2. The fluence sensitivity of the Milagro detector as a function of GRB duration (black line). The fluence estimate is for a $\frac{dN}{dE} \propto E^{-2.4}$ particle spectrum with no cutoff. The fluence is taken to be the integral of the GRB energy above the median energy of the Milagro detector (typically a few TeV). Also plotted (the blue points) are the measured fluences and durations of an ensemble of BATSE detected GRBs.

decade in increasing probability. For the first three plots, the probabilities for GRB candidate positions with less than 2 events are excluded by the search algorithm, leaving a the high probability region vacant. The kink in the probability distributions for the final 2 plots at $log_{10}P=-4$ is due to the increase in the search grid density for regions of large excess employed by the second search algorithm described above. A GRB on these plots would show up as a cluster of points with very low probability (high significance) substantially separated to the from the statistical background. No GRBs were found in the initial search of this data set.

4 Sensitivity of Milagro to GRBs

Although, the flux of γ -ray from GRBs is almost certainly low at energies greater than 100 GeV, the large effective area of Milagro and it's large aperture make Milagro's sensitivity to GRB fluence superior to that of EGRET and comparable to that of BATSE. Figure 2 shows the fluence sensitivity of Milagro (at the TeV scale) vs the duration of the GRB compared to an ensemble of measured 100 keV scale GRB fluences and duration by BATSE.

5 Conclusion

A search was conducted for GRBs in a subset of the Milagro data on timescales ranging from $250\mu s$ to 40s. The search yielded no GRB detections. The calibration and the reconstruction algorithms have been substantial improved since the collection of these data. Updated results and upper limits will be presented at the conference.

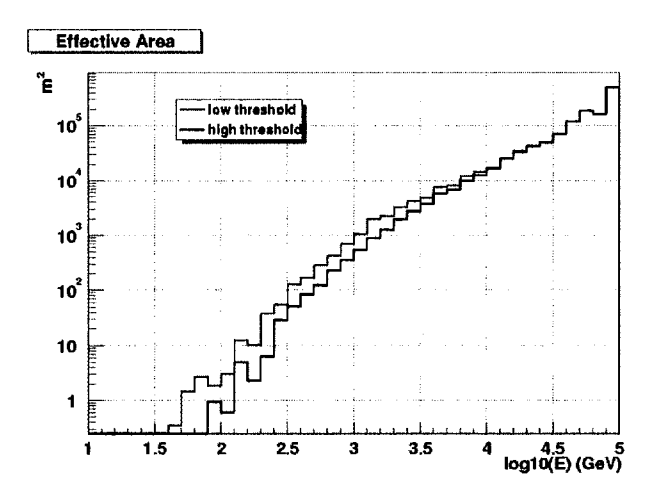


Fig. 3. The effective area of the Milagro detector as a function of Energy for a or current trigger (High Threshold) and our planned trigger upgrade (Low Threshold).

In the event that Milagro should observe GRBs, we are implementing online GRB search software. The system will search the Milagro data as it is collected and conduct the search described in this paper for GRBs. Should a GRB occur within Milagro's sensitivity, the system will be capable identifying it within 4s of the completion of the burst. Milagro could provide prompt notification of GRBs with position localization of about 0.2°. A TOO proposal to rapidly follow up a future Milagro GRB detection with the RXTE satellite has been approved.

During 2001, the Milagro detector will be substantially upgraded to increase it's sensitivity to GRBs. A critical limitation to the detection of GRBs at energies greater than \approx 50 GeV is the absorption of VHE γ -rays by the IR background radiation. To increase our sensitivity, it is therefore vital to lower the energy threshold of the instrument. Milagro, as currently functioning, triggers when 50 of the 450 top layer PMTs are hit within a 200ns window. Our detector simulations show that we can reliably reconstruct the direction of γ -ray induced showers with as few as 25 hits in the top layer of PMTs. Unfortunately, backgrounds from single muon triggers prevent us from lowering our trigger threshold allowing the detector to trigger on showers with lower energies. A smart trigger card has been built to identify and veto on the single muon background while preserving the air-shower events and will be installed during the Summer of 2001 (Hays and Noyes 2001). Figure 3 shows the effective area of Milagro as a function of energy for a the current Milagro trigger (High Threshold) and the planned Milagro trigger (Low Threshold). The increase in area while nominal at energies greater then 1 TeV is quite substantial at energies below 300 GeV. This upgrade will substantially increase our sensitivity to GRBs with redshifts greater than z = 0.3.

Additionally, an array of outrigger tanks (Shoup 1999) is being constructed around the Milagro detector. The array will improve the angular resolution and the γ -hadron separation of Milagro providing an overall increase in the flux sensitivity of about a factor of 2.

Acknowledgements. (add standard acknowledgment of DOE, LANL, NSF etc here)

References

Atkins et al., ApJL, 533, L119.
Benbow, W. et al, ICRC 2001.
Dermer, C.D., Böttcher, M., Chiang, J., ApJ, 537, 255-260.
Dingus, B.L., Catelli, J.R. & Schneid, E.J. 1998, 4th Huntsville GRB Symposium, AIP, 428, 349
Esposito, J.A., et al, ApJS 123, 203.
Hays E., Noyes D. et al Gamma 2001 Proceedings

Paciesas, W.S. et al, ApJS 122, 465. Sinnis, G. et al, ICRC 2001. Shoup, A. et al, ICRC 1999. Sullivan, G. et al, ICRC 2001.

Single Hadrons in Milagro and the Spectrum of Cosmic Ray Protons

Gaurang B. Yodh for the Milagro Collaboration

Department of Physics and Astronomy, University of California Irvine, Irvine, CA, USA, 92697-4575

Abstract.

Single unaccompanied hadrons can be used to probe the shape and intensity of the primary cosmic ray proton spectrum. The Milagro detector is a very large calorimeter with an effective area for the detection of unaccompanied hadrons of 2000 m² and a thickness of 6 meters (7 interaction lengths and 16 radiation lengths) to sample primary protons which survive to Milagro level without interacting in the atmosphere. The response of the shower layer (PMTs located below about 1.35 meter of water) is used to establish calorimeter penetration by single hadrons without accompanying shower particles and the hadron energy is estimated from the response of the PMTs located below 6 meters of water.

Criteria developed to select candidate single hadrons are described and distributions of observed signals are compared with simulations of the response of Milagro to single hadrons incident upon the pond.

1 Introduction

Single hadrons, unaccompanied by any shower particles, are an upper limit to the number of protons surviving at observation level without interaction. As the energy of the single hadron increases the limit approaches the true flux of surviving hadrons. A measurement of unaccompanied hadron flux as a function of energy can be used to infer the spectrum of primary cosmic ray protons over a wide energy range and in principle could determine the bend in the proton spectrum in the 100s of TeV energy range (F. Siohan et al., 1978 and T.K. Gaisser et al., 1977).

Single hadrons in Milagro are energetic hadrons which are incident upon the Milagro pond without accompanying shower particles. These energetic hadrons produce a nuclear-electromagnetic cascade in the water. The transverse extent of these cascades is limited in the shower layer to a narrow bundle and the main beam of Cherenkov light is only about

a meter and half wide for nearly vertical hadrons. The Milagro trigger requires that 50 or more tubes are hit. This 50 tube trigger is satisfied by single hadrons by some of the emitted Cherenkov light travelling nearly horizontally in the water and illuminating photo-multipliers(PMTS) away from the core of the cascade. This nearly horizontal light is produced by Cherenkov emission from multiply scattered low energy electrons in the cascade. Monte Carlo simulations of energetic single hadrons incident upon the pond with energies greater than 10 GeV show that these cascades satisfy the trigger requirements. This light, generated at the cascade, travels with speed of light in water (4.5 nanoseconds per meter). This feature provides a clean method for selecting triggers due to single hadrons. An estimate of the energy of the single hadron is obtained from the sum of the total number of photo-electrons detected in the top and the bottom layer, pesumtop(pt)+pesumbot(pb), called x hereafter.

We present a preliminary comparision of single hadron data with simulations which provides a validation of the method.

2 Method of Singleh hadron selection

The procedure to select out single hadron(SH) triggers consists of the following steps: (1) Find the tube with maximum number of photoelectrons detected(pes) in the top layer(maxtube), (2) calculate the time delay, t_i (ns), of all hit tubes with respect to the time of the maxtube and the distance of the tubes from the maxtube r_i (meters). (3) calculate the difference between t_i and the time it takes for light to travel in water to the tube from the maximum tube, $[t_i-4.5 r_i]$ and require its absolute value to be less than 20 ns and (4) calculate the fraction of hit tubes satisfying this condition to the total number of hit tubes, f. If f is greater than 0.9, the event is a good single hadron candidate. When this selection is applied to the data, about 0.5 percent of the events are selected.

A further selection is applied to make sure that the single hadron penetrated both layers and its trajectory was well contained within the pond. Simulations showed that with this

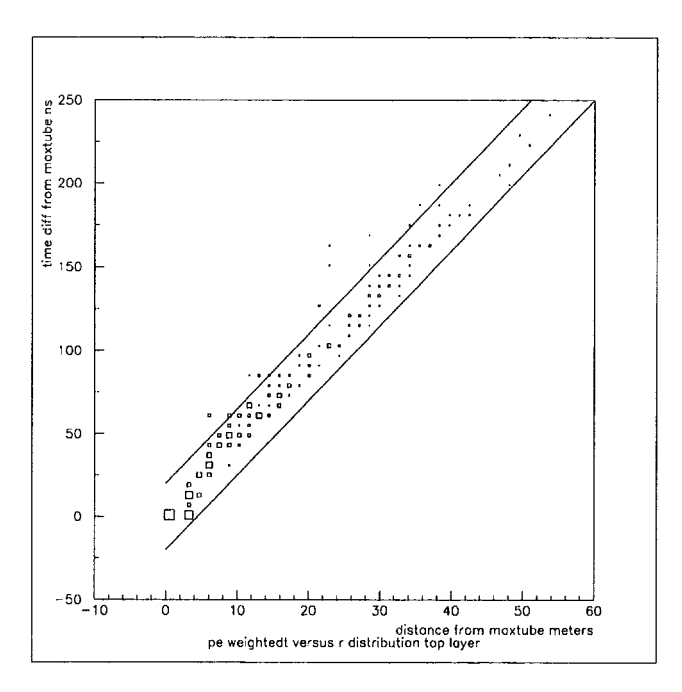


Fig. 1. Figure 1: Distribution of hits along the speed of light in water line for a selected single hadron candidate

selection we select single hadrons of energy above 100 Gev with high efficiency.

A plot of t_i versus r_i for a typical selected single hadron event is shown in Figure 1. The figure clearly shows that hits away from the maxtube lie along the speed of light in water line.

The distribution of hit pmts in the top and bottom layer weighted by the pes for each tube is shown in Figure 2 for the same selected hadron candidate. A clear indication of the collimated cascade structure is seen in the figure.

3 Energy determination

Single protons with energy greater than 50 GeV with a spectral index of -2.9 and with zenith angles less than 15 degrees were incident on Milagro were simulated. For each selected event we plot the relation between log10(x) and log10(E), where E is the energy of the proton in GeV in Figure 3.

The observed correlation is fitted to a straight line and the result is

$$x = 126E^{0.69 \pm 0.03} \tag{1}$$

For later use we call the exponent δ .

4 Observed single hadron spectrum

We are currently outputting single hadron files selected requiring that the fraction of hits in the speed of light in water band are greater than 90 percent of the total hits. For each of these events we estimate their zenith angle by geometry of the cascade as seen in top and bottom layers. We further

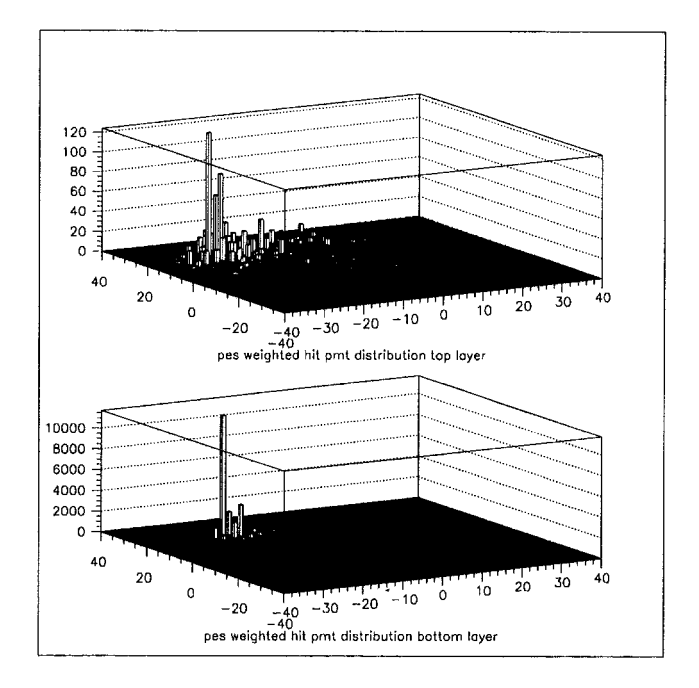


Fig. 2. Figure 2: Two dimensional display of pes weighted hit tubes in the top and bottom layers

require that the zenith angle so determined is less than 25 degrees. This should give us a sample of unaccompanied single hadrons in the pond. The observed spectrum of sum of total photoelectrons detected in the top and bottom layer, (pt+pb), of these selected events is given in Figure 4.

The fitted spectral index, is called β , where $\frac{dN}{dx} = B x^{-\beta}$ and x = (pt+pb). This is obtained using sufficiently high values of x so as not to be influenced by threshold effects clearly seen in Figure 2, and is found to be: $3.28\pm.07$. What does this tell us about the spectral index of the energy spectrum of single hadrons that it corresponds to? This is addressed next.

5 The relation of spectral indices

Let the spectral index of the energy spectrum of the single hadrons incident upon Milagro be γ , so that we can write

$$\frac{dN}{dE} = KE^{-\gamma} \tag{2}$$

The relation between x and energy is taken from Monte Carlo (see Figure 1) and written as

$$x = AE^{\delta} \tag{3}$$

One can easily show that the relation between γ , δ and β is

$$\beta = \frac{\gamma}{\delta} - \frac{1}{\delta} + 1 \tag{4}$$

From this we estimate the spectral index of the incident single hadrons in data to be approximately -2.6 with an uncertainty of about ± 0.2 . This value is quite reasonable and is

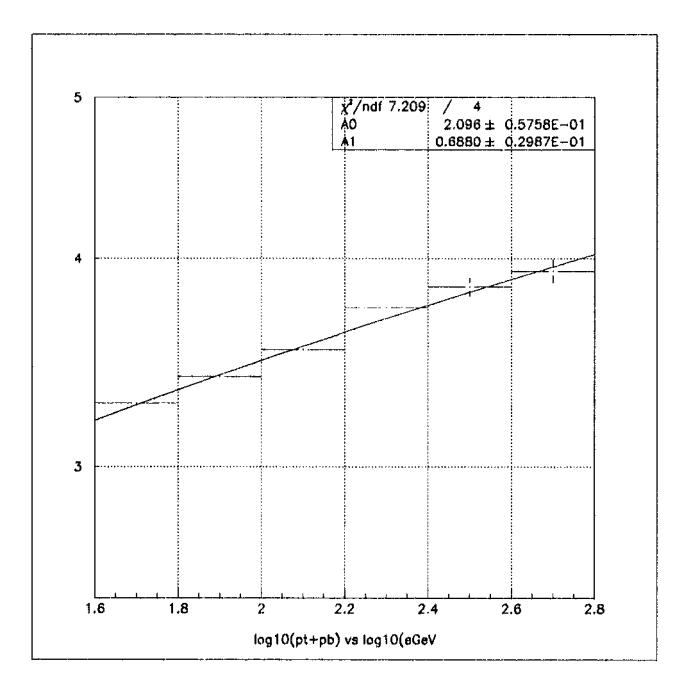


Fig. 3. Figure 3: Correlation of observed total pes and true energy in GeV

what is expected from solution of the coupled cascade equations for the hadronic cascade in the atmosphere. In this energy range where we expect scaling to hold in the fragmentation region and where the interaction cross section is almost energy independent(T.K.Gaisser, 1990) one expects the single hadron spectral index to reflect that of the primary cosmic rays provided that the energy resolution of is reasonably symmetric. These unaccompanied hadrons originate mostly from primary protons and helium nuclei, whose spectral indices in the 100 GeV energy range are -2.75 and -2.64 respectively.

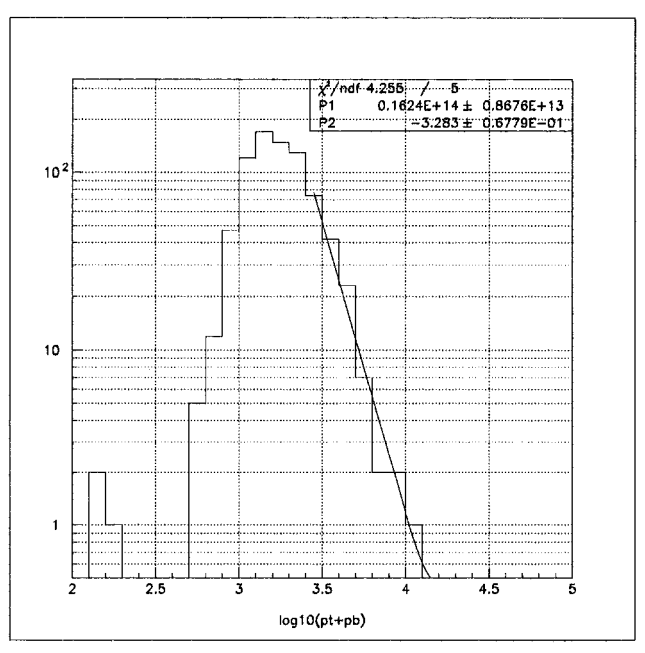
Acknowledgements. This work is supported by the US National Science Foundation, by DoE, by the LDRD program at LANL and the IGPP of the University of California.

References

F. Siohan et al., J. Phys.G; Nucl, Phys. 4, 1169, 1978.

T.K.Gaisser, F. Siohan and G.B.Yodh, J. Phys. G; Nucl. Phys. 3, L241, 1977.

T. K. Gaisser, Cosmic Rays and Particle Physics, Cambridge University Press, 1990.



.png

Fig. 4. Figure 4: Observed spectrum of total detected photoelectrons in top and bottom layer